# A new caged $Ca^{2+}$, azid-1, is far more photosensitive than nitrobenzyl-based chelators

Stephen R Adams[1], Varda Lev-Ram[1] and Roger Y Tsien[1,2,3]

**Background:** Photolabile chelators that release $Ca^{2+}$ upon illumination have been used extensively to dissect the role of this important second messenger in cellular processes such as muscle contraction and synaptic transmission. The caged calcium chelators that are presently available are often limited by their inadequate changes in $Ca^{2+}$ affinity, selectivity for $Ca^{2+}$ over $Mg^{2+}$ and sensitivity to light. As these chelators are all based on nitrobenzyl photochemistry, we explored the use of other photosensitive moieties to generate a new caged calcium with improved properties.

**Results:** Azid-1 is a novel caged calcium in which a fluorescent $Ca^{2+}$ indicator, fura-2, has been modified with an azide substituent on the benzofuran 3-position. Azid-1 binds $Ca^{2+}$ with a dissociation constant ($K_d$) of ~230 nM, which changes to 120 μM after photolysis with ultraviolet light (330–380 nm). $Mg^{2+}$ binding is weak (8–9 mM $K_d$) before or after photolysis. Azid-1 photolyzes with unit quantum efficiency, making it 40–170-fold more sensitive to light than caged calciums used previously. The photolysis of azid-1 probably releases $N_2$ to form a nitrenium ion that adds water to yield an amidoxime cation; the electron-withdrawing ability of the amidoxime cation reduces the chelator's $Ca^{2+}$ affinity within at most 2 ms following a light flash. The ability of azid-1 to function as a caged calcium in living cells was demonstrated in cerebellar Purkinje cells, in which $Ca^{2+}$ photolytically released from azid-1 could replace the normal depolarization-induced $Ca^{2+}$ transient in triggering synaptic plasticity.

**Conclusions:** Azid-1 promises to be a useful tool for generating highly controlled spatial and temporal increases of $Ca^{2+}$ in studies of the many $Ca^{2+}$-dependent biological processes. Unlike other caged calciums, azid-1 has a substantial cross section or shows a high susceptibility for two-photon photolysis, the only technique that confines the photochemistry to a focal spot that is localized in three dimensions. Azide photolysis could be a useful and more photosensitive alternative to nitrobenzyl photochemistry.

Addresses: [1]Department of Pharmacology, [2]Department of Chemistry and Biochemistry and [3]Howard Hughes Medical Institute, 310 Cellular and Molecular Medicine West, University of California San Diego, La Jolla, CA 92093-0647, USA.

Correspondence: Stephen R Adams
E-mail: sadams@ucsd.edu

**Key words:** azides, caged calcium, cerebellum, long-term depression, photolysis

Received: **30 July 1997**
Revisions requested: **1 September 1997**
Revisions received: **25 September 1997**
Accepted: **3 October 1997**

**Chemistry & Biology** November 1997, 4:867–878
http://biomednet.com/elecref/1074552100400867



## Introduction

The generation of controllable increases in intracellular free $Ca^{2+}$, $[Ca^{2+}]_i$, by photolysis of caged calcium chelators has become a standard technique in physiology and cell biology [1–4]. A high affinity photolabile $Ca^{2+}$ chelator is introduced into the cell as the predominant $Ca^{2+}$ buffer (at concentrations of a few millimolar) and irradiated with ultra-violet (UV) light to produce a weaker binding photoproduct, thus releasing $Ca^{2+}$. The starting affinity and the selectivity of the chelator for $Ca^{2+}$, degree of loading with $Ca^{2+}$, change in affinity for $Ca^{2+}$ upon photolysis, and the photosensitivity of the caged $Ca^{2+}$ govern the magnitude of the elevation in $Ca^{2+}$ attainable per flash of UV light. These properties of the currently available caged $Ca^{2+}$ chelators, nitr-5 [5], nitr-7 [5], dimethoxy (DM)–nitrophen [6], and nitrophenyl (NP)–EGTA [7] are summarized in Table 1.

All the currently available $Ca^{2+}$ chelators exploit the two-nitrobenzyl photochemistry [2,8,9] used by most caged compounds to either electronically (e.g. the nitr series of caged $Ca^{2+}$) or sterically (DM–nitrophen and NP–EGTA) reduce the binding of $Ca^{2+}$ to the chelator. This leads to a limit on the overall light sensitivity of such chelators as these groups have low absorbancy ($\varepsilon \sim 5000\ M^{-1}\ cm^{-1}$) and modest quantum efficiencies (0.20 or less). Low photosensitivities limit the magnitude and duration of the $Ca^{2+}$ jump attainable, particularly because unphotolyzed $Ca^{2+}$-free chelator can rebind the photoreleased $Ca^{2+}$. Higher light intensities to compensate for low photosensitivity are often intrinsically damaging to the cells or technically difficult to deliver. Low photosensitivity is a major problem with two-photon uncaging of photoreleasable compounds [10], a technique, in which two infra-red photons replace a single ultra-violet photon, that promises far greater spatial

**Table 1**

**Properties of nitr-5, nitr-7, DM-nitrophen, NP-EGTA and azid-1.***

| Photolabile chelator | $K_d$ for $Ca^{2+}$ (μM) before hυ | $K_d$ for $Ca^{2+}$ (μM) after hυ | $K_d$ for $Mg^{2+}$ (mM) before hυ | $K_d$ for $Mg^{2+}$ (mM) after hυ | Quantum yield† Q | Extinction coefficient†† ε ($M^{-1}$ $cm^{-1}$) | Light sensitivity§ εQ ($M^{-1}$ $cm^{-1}$) |
|---|---|---|---|---|---|---|---|
| nitr-5# | 0.145 | 6.3 | 8.5 | 8 | 0.035 | 5500 | 190 |
| nitr-7# | 0.054 | 3.0 | 5.4 | 5 | 0.042 | 5500 | 231 |
| DM-nitrophen¶ | 0.005 | 3000 | 0.005 | 3 | 0.18 | 4330 | 780 |
| NP-EGTA¥ | 0.080 | 1000 | 9.0 | ~9 | 0.23 | 974 | 224 |
| azid-1 | 0.23 | 120 | 7.6 | ~9 | 1 | 33,000 | 33,000 |

*Dissociation constants ($K_d$) values before and after photolysis are given for pH 7.0–7.5 and 0.1–0.15 M ionic strength and 22 ± 2°C, except for DM-nitrophen and NP-EGTA which have values that are pH sensitive in this range so they were determined at pH 7.2. †The quantum yield is the efficiency of photolysis of the $Ca^{2+}$-bound chelator. ††The extinction coefficient of the $Ca^{2+}$ form of the chelator at its dominant peak at the longest wavelength, except for NP-EGTA which is the recorded value at 347 nm. §The product of the extinction coefficient and quantum yield is a measure of the light sensitivity of the photolabile chelator and is reported for the $Ca^{2+}$-bound species. #From [5]; ¶from [6]; ¥from [7].

control but has suffered from the drastically inadequate two-photon cross section (or low photolysis susceptibility) of existing nitrobenzyl compounds.

The ideal caged $Ca^{2+}$ would combine the high $Ca^{2+}$:$Mg^{2+}$ selectivity, pH insensitivity and fast buffering kinetics of the BAPTA (1,2-bis(2-aminophenoxy)ethane-*N*,*N*,*N*′*N*′-tetraacetic acid)-based nitr series of chelators, the large change in $Ca^{2+}$ affinity of DM-nitrophen and NP-EGTA with increased light sensitivity through higher quantum efficiencies and/or extinction coefficient. The $Ca^{2+}$ affinity of the unphotolyzed chelator should match or be slightly less than typical $[Ca^{2+}]_i$ resting levels to provide maximal buffering power and therefore control of pre-illumination $Ca^{2+}$ levels. After photolysis, final $[Ca^{2+}]_i$ of tens to hundreds of micromolar should be attainable to match the physiological levels reached in microdomains immediately below membrane $Ca^{2+}$ channels [11].

A newly developed caged $Ca^{2+}$, azid-1, appears to fulfil most of these criteria. Azid-1, the 3-azido derivative of fura-2 [12], has the high $Ca^{2+}$:$Mg^{2+}$ selectivity of BAPTA chelators and decreases its $Ca^{2+}$ affinity 500-fold upon photolysis (Figure 1). It has an extinction coefficient of 33,000 $M^{-1}cm^{-1}$ and quantum yield of 1.0, making it 40–170 times more light sensitive than previous caged $Ca^{2+}$ and it is also capable of releasing $Ca^{2+}$ at rates sufficient for most biological experiments.

## Results

### Photochemical and synthetic strategy

To investigate a wider range of photochemical reactions in the manipulation and measurement of $Ca^{2+}$-dependent processes in biology, we explored the properties of aromatic azides. $Ca^{2+}$ chelators containing an azido substituent in the 3-position of a benzofuran were selected for their similarity to the fura family of fluorescent $Ca^{2+}$ indicators [12] and because of their comparative ease of synthesis. An azide derivative of fura-2, named azid-1, was prepared by the steps shown in Figure 2. A key intermediate was the salicylnitrile (**6**) derivative of BAPTA which was synthesized from the salicylaldehyde benzyl ether (**3**) via dehydration of the intermediate oxime (**4**) by phosgene iminium chloride. Reaction of the salicylnitrile with ethyl 2-(chloromethyl)oxazole-5-carboxylate generated a derivative (**7**) of fura-2 containing a 3-amino group on the furan ring. Two interesting products were produced from **7**. Simple saponification gave 3-amino-fura-2, a $Ca^{2+}$ indicator with strong fluorescence like its parent fura-2 but with a large blue shift in emission from 485 nm to 433 nm upon

**Figure 1**

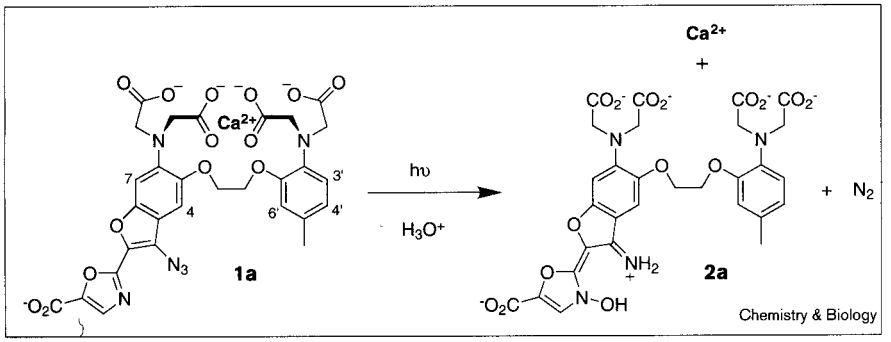


Photolysis of the $Ca^{2+}$ complex of azid-1 (**1a**) leading to the formation of an amidinium product (**2a**) and photorelease of $Ca^{2+}$.

**Figure 2**

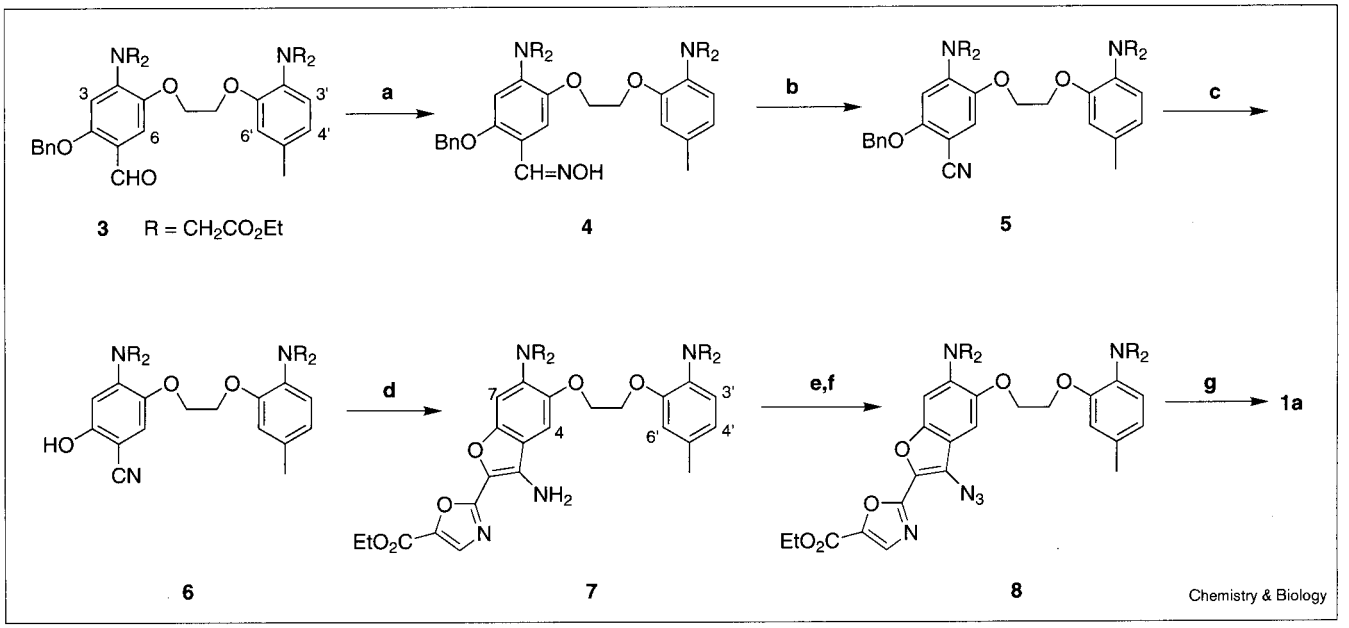


Synthesis of azid-1 (**1a**, see Figure 1). Reagents: **a**, $NH_2OH$, NaOAc, dioxane-MeOH; **b**, $Me_2N^+ = CCl_2$ $Cl^-$, $CHCl_3$; **c**, $H_2$, Pd-C, HOAc; **d**, ethyl 2-(chloromethyl)oxazole-5-carboxylate, $K_2CO_3$, DMF; **e**, $NOHSO_4$, HOAc-$H_2SO_4$; **f**, $NaN_3$, $H_2O$; **g**, KOH, dioxane-MeOH.

binding $Ca^{2+}$ (with a dissociation constant of 0.1–0.2 μM), analogous to indo-1 [12] rather than fura-2 which has a negligible emission shift. The sensitivity of the emission wavelengths of 3-amino-fura-2 to $Ca^{2+}$ binding probably results from the electron-donating properties of the amino substituent, which makes the excited state relatively electron-rich, like indo-1, so that the $Ca^{2+}$-complex is not so prone to dissociate in the excited state.

Diazotization of ester **7** to form a diazonium salt and displacement with azide gave the pentaethyl ester of azid-1 (**8**) in good yield. Saponification of the esters with potassium hydroxide gave the desired product (**1a**), which was particularly light sensitive and unexpectedly lost affinity for $Ca^{2+}$ when photolyzed. Azid-1 was therefore investigated further as a potential caged $Ca^{2+}$.

### Spectral properties, $Ca^{2+}$ binding, photolysis and quantum yield of azid-1

The absorbance spectra of azid-1 with and without $Ca^{2+}$ were similar to those of the parent chelator fura-2, but were red-shifted by about 10 nm as would be expected from the incorporation of an azide group into an aromatic system [13]. $Ca^{2+}$-free azid-1 absorbed maximally at 372 nm with an extinction coefficient of 27,000 $M^{-1}$ $cm^{-1}$, compared to values of 362 nm and 27,000 $M^{-1}$ $cm^{-1}$ for fura-2 [12]. In the presence of $Ca^{2+}$, the spectrum of azid-1 shifted 30 nm to shorter wavelengths giving a maximal absorbance of 33,000 $M^{-1}$ $cm^{-1}$ at 342 nm compared to 33,000 $M^{-1}$ $cm^{-1}$ at 335 nm for fura-2. The $Ca^{2+}$ affinity of azid-1 before photolysis was determined to be 230 nM by measuring absorbance spectra in an EGTA-buffered solution that was set to various free $Ca^{2+}$ concentrations (Figure 3a). A Hill plot of this spectral change gave a gradient of 1, indicating a 1:1 complex is formed between azid-1 and $Ca^{2+}$. The slight weakening of $Ca^{2+}$ binding probably results from increased electron withdrawal at the chelating amino group by the conjugated electronegative azide. The replacement of the benzofuran 3-hydrogen of fura-2 by an azido group therefore had only small and rationalizable effects upon the absorbance spectra and metal binding of the resulting molecule, azid-1.

Upon UV illumination, however, azid-1 did not fluoresce like fura-2 but underwent the irreversible spectral changes shown in Figure 3b and c. Thus, following irradiation at 365 nm, in zero $Ca^{2+}$, the main absorbance peak shifted cleanly (with sharp isosbestic points) to a longer wavelength (400 nm) with a similar high extinction coefficient. The subsequent addition of $Ca^{2+}$ produced a shift to the blue (to about 350 nm) and a large decrease in absorbance. A $Ca^{2+}$ titration of the photoproduct revealed, unexpectedly, that the $Ca^{2+}$ affinity was reduced over 500-fold to about 120 μM (Figure 3d). Photolysis of azid-1 in $Ca^{2+}$ resulted in a similar spectrum indicating the same photoproduct was formed with and without $Ca^{2+}$ (Figure 3b). The efficiency of this photochemical reaction was very high; quantum yields of 1.3 and 0.9 were measured from the absorbance changes in the presence or absence of $Ca^{2+}$ respectively. The value of >1 (i.e. more than 1 product molecule formed per photon

absorbed) probably reflects errors or uncertainties in the UV-light intensity measurement, the finite spectral width of the irradiating beam at 365 nm, or in the extinction coefficient of $Ca^{2+}$ bound azid-1 at 365 nm, at the edge of

**Figure 3**

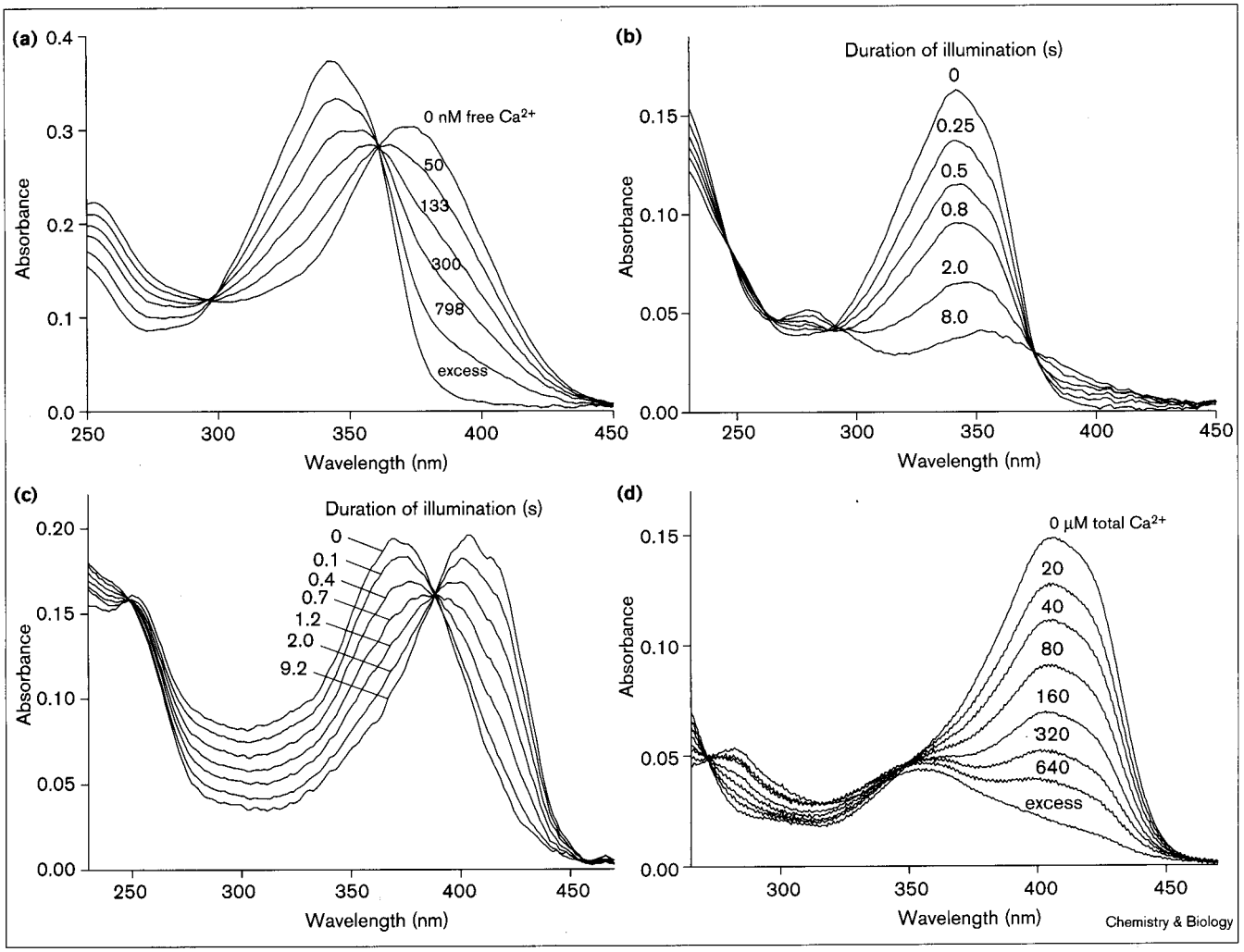


**(a)** Absorbance spectra of unphotolyzed azid-1 as a function of free [$Ca^{2+}$]. The titration was performed at 22°C by using 10 ml of 100 mM KCl, 10 mM K·MOPS, 10 mM $K_2H_2$·EGTA and 11 µM azid-1 as starting materials, adjusting the pH to 7.14, recording the spectrum, and then discarding 1.0 ml of this solution and replacing it with 1.0 ml of 100 mM KCl, 10 mM K·MOPS, 10 mM $K_2Ca$·EGTA and 11 µM azid-1, readjusting the pH to 7.14, and recording the spectrum which was then in 9 mM $K_2H_2$·EGTA. Subsequent iterations to reach $n$ mM $K_2Ca$·EGTA, (10−$n$) mM $K_2H_2$·EGTA, $n = 2–10$, were performed by discarding 10.0/(11−$n$) ml and replacing it with equal volumes of the 10 mM $K_2Ca$·EGTA, 11 µM azid-1 stock. After $n = 10$ had been reached to give a free $Ca^{2+}$ between $10^{-5}$ and $10^{-4}$ M, addition of excess 1 mM $CaCl_2$ had a small additional effect on the spectrum. For clarity, only six spectra are included in the figure, $n = 0$, 2, 4, 6, 8 and excess. Each spectrum is labeled with the calculated free [$Ca^{2+}$] imposed by the EGTA buffer, assuming a log effective stability constant [35] of 6.70 at pH 7.14. **(b)** Absorbance spectra of azid-1 undergoing photolysis in the presence of $Ca^{2+}$. Azid-1 was dissolved at 5 µM in 100 mM KCl, 10 mM MOPS, 12 mM Tris, 1 mM $Tris_3$·EDTA, 3 mM $CaCl_2$ pH 7.5. Spectra were obtained after 0.05, 0.1, 0.25, 0.4, 0.5, 0.8, 1.3, 2.0, 4.0 and 8.0 s of 365 nm illumination at $1.6 \times 10^{-8}$ einstein $cm^2$ $s^{-1}$ from the Spectroline line. For clarity, only the recorded at spectra 0, 0.25, 0.5, 0.8, 2.0 and 8.0 s have been reproduced here. The 4.0 s and 8.0 s spectra were identical, confirming that photolysis was complete after those times. Solutions were at 22 ± 2°C. **(c)** Absorbance spectra during photolysis of azid-1 in the absence of $Ca^{2+}$. The method was as described in (b) except that the solution contained no $CaCl_2$, and the spectra were measured after 0, 0.1, 0.2, 0.4, 0.7, 1.2, 2.0, 3.0, 5.0 and 9.2 s of illumination at $1.6 \times 10^{-8}$ einstein $cm^2$ $s^{-1}$ from the Spectroline line. The last two spectra were identical confirming completion of photolysis. For clarity, the 3.0 and 5.0 s spectra have been omitted. **(d)** Absorbance spectra of photolyzed azid-1 as a function of total [$Ca^{2+}$]. The photoproduct was produced by irradiating a 4 µM solution of azid-1 in 100 mM KCl (Ultrex grade; J.T. Baker Chem Co., Phillipsburg, NJ), 10 mM K·MOPS, pH 7.30, using the Spectroline lamp at 365 nm until completion. The titration was performed by the stepwise addition of concentrated $CaCl_2$ solution to attain a total [$Ca^{2+}$] in the cuvet of 5, 10, 20, 40, 80, 160, 320, 640, 21,600 and 61,600 µM, and successively recording the absorbance spectrum. For clarity, only the spectra corresponding to 0, 20, 40, 80, 160, 320, 640 and 21,600 µM are shown here. The spectra at 21,600 and 61,600 were almost identical indicating complete saturation of the photoproduct by $Ca^{2+}$ was achieved.

the absorbance peak. In contrast to the large change in $Ca^{2+}$ affinity upon photolysis, the $Mg^{2+}$ affinity remained essentially unchanged at about 8 mM. The photoproduct itself was not fluorescent, although slight impurities of 3-amino-fura-2 sometimes made solutions of azid-1 appear fluorescent before and after photolysis. In different preparations of azid-1, the concentration of this contaminant varies from 3–4% of the azid-1, that is 30–40 μM of indo-1-like indicator per 1 mM azid-1. Like most aromatic azides [14], azid-1 is susceptible to reduction to the fluorescent 3-amino-fura-2 by thiol anions at alkaline pH, particularly by dithiols such as dithiothreitol. Azid-1 reacts with 2-mercaptoethanol (10 mM) at physiological pH and room temperature with a half-life of 1–2 h (data not shown). Contact with such thiols should therefore be kept to a minimum.

**Nature of the photoproducts**

As the photolysis of aromatic azides can generate a variety and mixture of photoproducts via the highly reactive nitrene intermediate, it was important to analyze and identify the product(s) resulting from irradiation of azid-1. Separation of the reaction mixture produced by photolysis of 50 μM to 10 mM azid-1 pentapotassium salt at pH 7 with or without $Ca^{2+}$ by reverse-phase thin layer chromotography (TLC), reverse-phase high performance liquid chromotography (HPLC) or capillary electrophoresis indicated only one major product, that was non-fluorescent was formed (data not shown). This product was stable at physiological pH for at least several hours, considerably more polar than azid-1 as judged by retention on reverse-phase HPLC, and slightly less negatively charged at pH 7 as judged by its electrophoretic behavior. Raising the pH caused an initially reversible spectral shift of the photoproduct to shorter wavelengths; this transition had a $pK_a$ of about 10.5. Prolonged standing at high pH made the hypsochromic shift irreversible. A similar product appeared to result from hydrolysis of the photoproduct at pH 4.5 at room temperature over several hours. We hoped to separate and identify the products more easily by photolyzing large amounts of azid-1 pentaethyl ester in organic solvents, but more complex and different products were produced. Photolysis of azid-1 pentapotassium salt in methanol gave similar spectral shifts and loss of $Ca^{2+}$ affinity as occurred in water, but the product was still highly charged and difficult to analyze by chromatography and mass spectroscopy.

The reaction could also be conveniently monitored by $^1H$-nuclear magnetic resonance (NMR) by photolyzing 5 mM azid-1 at pH 7 in $D_2O$ in the absence of $Ca^{2+}$ in a NMR tube and acquiring spectra at various time points. Again, a fairly clean transformation to one product was observed with most proton resonances only undergoing modest shifts. Two major shifts occurred, involving the aromatic proton (H-7) and acetate protons ($N\text{-}CH_2CO_2^-$) adjacent to the benzofuran amino group with an upfield shift of 1.1 ppm and a downfield shift of 0.5 ppm respectively. The resulting spectrum is similar to those of BAPTA chelators bearing strong electron-withdrawing groups (such as aldehydes or nitrile groups e.g. **6**) para to the amino group and is consistent with the observed weakening of $Ca^{2+}$ binding. There was no indication of nitrene insertion (formed by loss of $N_2$ from the azido group) into the $Ca^{2+}$ binding site or the ring expansions found with many phenyl azides.

The most revealing approach eventually was to apply electrospray mass spectrometry to **1b** (Figure 4, $M = CH_3$), a truncated model of azid-1 in which the photochemically irrelevant bis(carboxymethyl)aminophenoxyethoxy moiety was replaced by a simple methoxy substituent, to aid volatilization and remove any complications of $Ca^{2+}$ binding. Compound **1b** showed the same changes in absorbance upon photolysis as azid-1, but it bound $Ca^{2+}$ with only millimolar affinity before photolysis. The compound **1b** was prepared by an analogous synthetic route [12] to that described for azid-1 but starting with 2-methoxy-5-(benzyloxy)nitrobenzene. Before photolysis, the major peak had a molecular ion of 430.2, corresponding to the singly charged parent molecule; a minor peak at 402.1 was interpreted as a loss of $N_2$, presumably by thermolysis during volatilization. Photolysis of **1b** in water gave a peak at 420.1, consistent with addition of water after initial expulsion of $N_2$. When the photolysis was conducted in methanol, the product had a mass of 434, confirming that a molecule of solvent had been added. Treatment of the 420.1 Da aqueous photoproduct with aqueous 1 M-triethylamine at room temperature overnight yielded the final hydrolysis product with a mass of 421.1. The methanol photoproduct was stable to aqueous triethylamine but under mildly acidic conditions (1 M acetic acid at room temperature overnight) gave a 435 Da product.

A reaction scheme consistent with all these results is shown in Figure 4 and involves initial loss of $N_2$ to generate a nitrene **9**. This highly reactive intermediate reacts with solvent water, probably via nitrenium ion **11**, to form a vinylogous N-hydroxyamidine **14** that protonates at pH 7 to give **2**. The delocalized positive charge of **2** is conjugated with and withdraws electron density from the amino group involved in $Ca^{2+}$ binding, leading to a large decrease in affinity. It seems reasonable that amidinium **2** should have a $pK_a$ of 10.5 and absorb at longer wavelengths than its conjugate base **14**. The positive charge on **2** is consistent with its reduced retention on reverse-phase HPLC or TLC and its decreased overall negative charge on capillary electrophoresis. Upon prolonged alkaline hydrolysis, the imine should hydrolyze to a carbonyl group in **20** with a gain of 1 Da as observed. Generation of the nitrene **9** in methanol should give the analogous N-methoxyamidine **15** which hydrolyzes to **21**, consistent with the mass spectra.

**Figure 4**

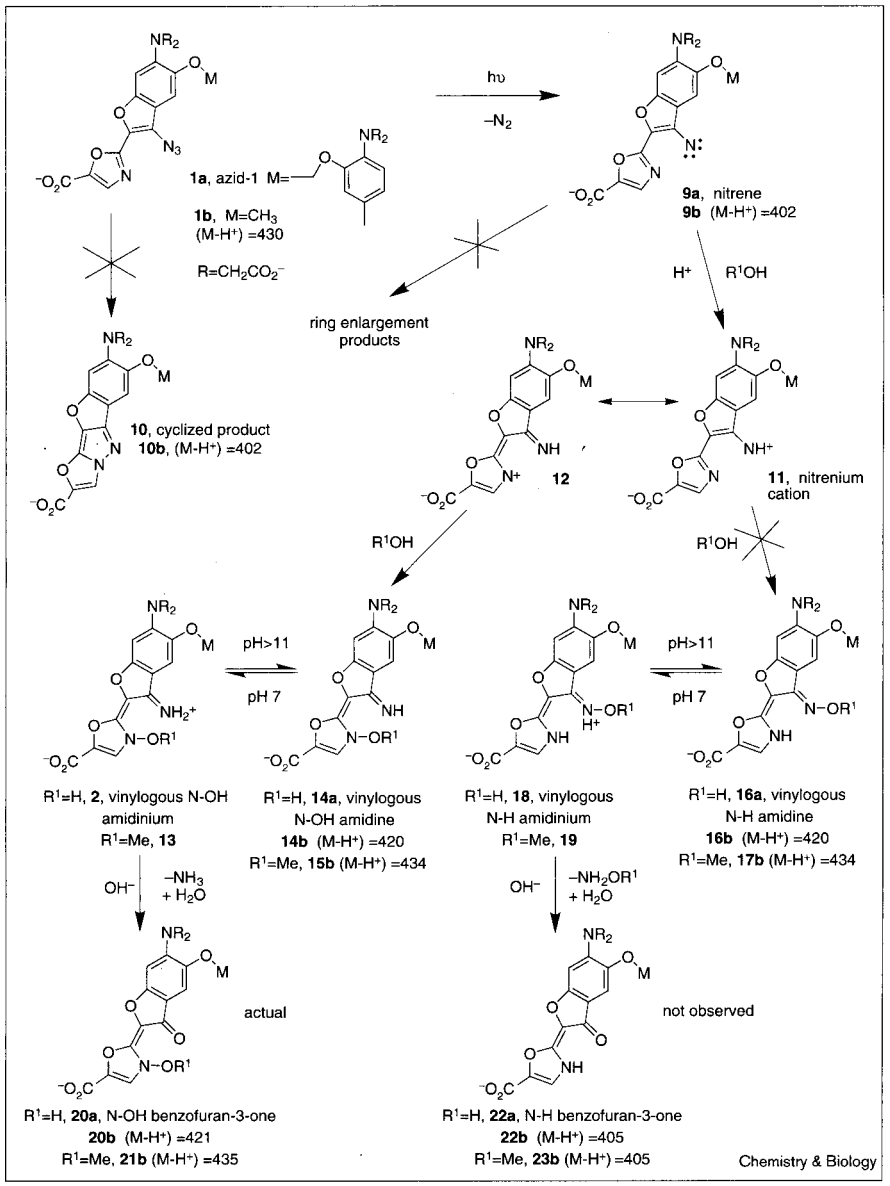


A possible mechanism for the photolysis of azid-1 (**1a**) and a model compound (**1b**), and the reaction of the putative photoproduct with MeOH or water at pH 7 and subsequent alkaline hydrolysis. See the Results and Discussion sections for details.

### Flash photolysis kinetics *in vitro*

For use as a caged $Ca^{2+}$ in many biological systems, azid-1 should release $Ca^{2+}$ rapidly (within a millisecond) following a light flash. The proposed mechanism for generating decreased $Ca^{2+}$ binding involves dark reactions which could be rate-limiting. To determine the rate of $Ca^{2+}$ release following flash photolysis, we used the fluorescent $Ca^{2+}$ indicator fluo-3 which permits monitoring of the $Ca^{2+}$ concentration at wavelengths that do not photolyze azid-1. The kinetics of $Ca^{2+}$ binding to fluo-3 have been estimated to be $> 10^9\ M^{-1}s^{-1}$ [15] and therefore should not limit the detection of $Ca^{2+}$ release under the conditions used (fluo-3 concentration of 0.1 mM). Following a brief flash (duration < 1 ms) of a mixture of azid-1, fluo-3 and $Ca^{2+}$, fluo-3 fluorescence increased to a new level with kinetics that were faster than the time-resolution of the instrument indicating the release of $Ca^{2+}$ from photolyzed azid-1 is complete within 2 ms (data not shown). Control experiments omitting azid-1 and/or $Ca^{2+}$ failed to give any changes in fluorescence.

### Biological testing of azid-1

Azid-1 is biologically useful because it can be used to demonstrate the role of $Ca^{2+}$ in synaptic plasticity of the cerebellum. Long-term changes in synaptic efficacy are thought to be the neuronal basis for learning and memory. In the cerebellum, long-term depression (LTD) is defined as the reduction in synaptic transmission between parallel

fibers and Purkinje cells resulting from simultaneous presynaptic activity and postsynaptic depolarization. We studied LTD in acute rat cerebellar slices using the whole-cell patch technique [16] which permits monitoring of the synaptic currents of the Purkinje cell while simultaneously introducing azid-1 by perfusion. Previously, we have demonstrated that NO is an essential participant in LTD induction and that it is produced outside the Purkinje cells as a result of parallel fiber activation. NO acts inside the Purkinje cell in concert with a depolarization-induced $Ca^{2+}$ transient to induce LTD [16]. Simultaneous parallel-fiber stimulation and depolarization (at a frequency of 1 Hz) for 30 s (Figure 5, protocol i) were unable to induce LTD as they normally would have in the absence of azid-1 [16,17] because unphotolyzed azid-1 is a high affinity $Ca^{2+}$ buffer and should mimic BAPTA in preventing LTD induction. When uncaging was synchronized with parallel-fiber stimulation over a similar 30 s period (protocol ii), however, LTD promptly resulted (n = 4). Thus, photoreleased $Ca^{2+}$ is sufficient to replace climbing fiber activity and depolarization, and the elevation of $[Ca^{2+}]_i$ is the only essential function of depolarization in inducing LTD in mature Purkinje cells in slices. Experiments using azid-1 gave similar results to those using another caged calcium, nitr-7 [5] except light flashes of much shorter duration (50–100 ms compared to 500 ms for nitr-7) were sufficient to induce LTD.

## Discussion

### Photochemical mechanism of azid-1

The majority of caged compounds (and all previous versions of caged $Ca^{2+}$) utilize the photochemistry of 2-nitrobenzyl groups in their photorelease mechanism. Other photochemical groups have been used more rarely. For example, diazo chelators [18] use the Wolff rearrangement of diazoketones to generate a $Ca^{2+}$ chelator with an increased affinity upon photolysis. Benzoin esters of ATP [19] release the nucleotide triphosphate upon UV illumination with the formation of a phenylbenzofuran photoproduct. The photochemistry of azides has been extensively studied from a physical and chemical standpoint but few applications have been reported to be pertinent to designing new caged compounds. Photo-affinity labeling [14,20], a technique used extensively in biology, frequently involves the photolysis of an azido group in a ligand to covalently tag a macromolecular receptor. Most aromatic azides react upon photolysis to produce a wide variety of end products resulting from ring expansion, direct insertion into saturated and unsaturated bonds, or self-reaction, however. Such behavior results from the highly reactive nitrene intermediate which rapidly reacts with many neighboring chemical groups [21]. Coupling such photochemistry to the photorelease of biologically active compounds is difficult, although an azide-based

**Figure 5**

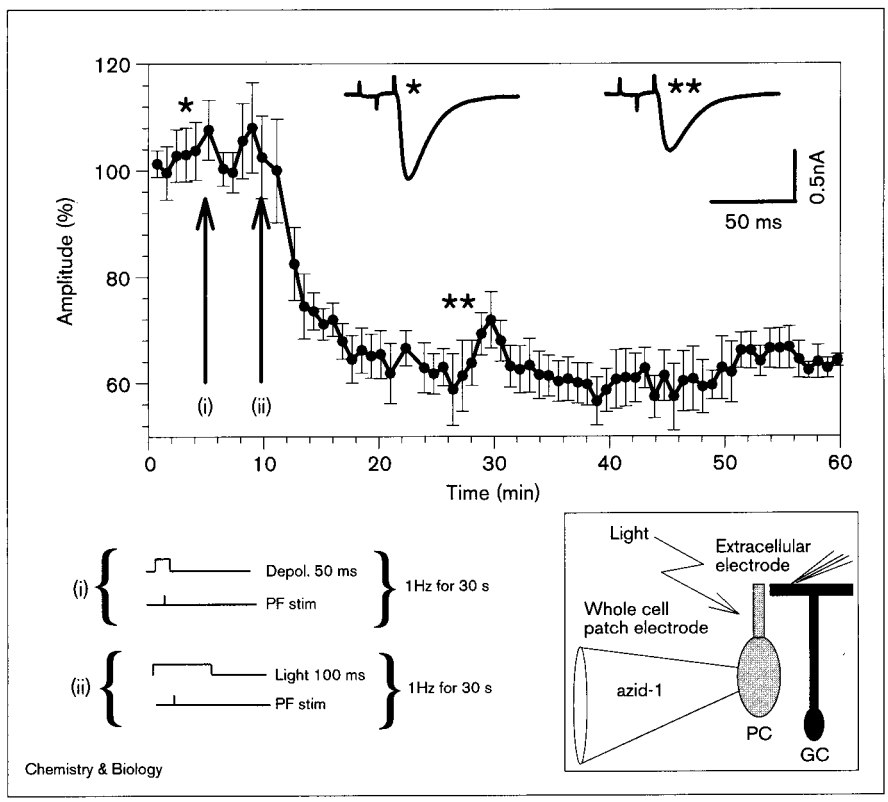


Induction of cerebellar long-term depression by uncaged $Ca^{2+}$ in conjunction with parallel-fiber stimulation. Excitatory postsynaptic currents (EPSCs) in a Purkinje neuron were monitored using whole-cell patch recording. Each EPSC trace is the average response from four cells and each point on the graph is an average of ten EPSC peak amplitudes from consecutive parallel-fiber stimuli delivered at 0.2 Hz (a test frequency too low to cause plasticity), normalized to the pretraining EPSC amplitude and averaged over all cells. Error bars represent the standard errors of each group. The patch pipette included 2 mM azid-1. Simultaneous parallel-fiber stimulation (PF stim) and depolarization (depol) at 1 Hz for 30 s, a standard training protocol (i) for eliciting long-term depression, was ineffective because unphotolyzed azid-1 buffered the $[Ca^{2+}]_i$ elevation. Before protocol (ii), azid-1 was reloaded with $Ca^{2+}$ from depolarization-induced $[Ca^{2+}]_i$ transients. When photolytic release of $Ca^{2+}$ by 100 ms flashes of 365 nm light (1 Hz for 30 s, protocol ii) coincided with parallel-fiber stimulation (1 Hz for 30 s), long-term depression was induced (i.e. a lasting reduction in EPSC amplitude to 62 ± 11% of its value just before training, a depression significant at the $p = 0.0031$ level by the one-tailed $t$ test). Insets show typical averages of ten consecutive EPSC traces from the times indicated by *,**. PC, Purkinje cell; GC, granule cell; PF, parallel fiber.

photoremovable protecting group for carboxylic acids has been reported [22]. One class of aromatic azides containing ortho unsaturated substituents such as C = O and $NO_2$, however, photolyze or thermolyze to single products in high yield via a concerted pericyclic mechanism without direct formation of a nitrene. The products result from insertion into the neighboring group and such reactions have been studied extensively [23].

Azid-1 is an azide-substituted derivative of the fluorescent $Ca^{2+}$ indicator fura-2, in which the imine bond (-C = N-) of the oxazole ring appears suitably sited for insertion. Such a photolysis mechanism would involve the initial loss of $N_2$ from the azido group followed by formation of a novel ring system (**10**, Figure 4) in which the benzofuran is fused to the oxazole through a pyrazole. Similar reactions have been reported for analogous classes of compounds such as 2-(2-azidophenyl)pyridine and 2-azidobenzylidene derivatives and result in the fusion of one or two 6-membered rings to a 5-membered heterocycle [13,24]. Surprisingly this mechanism apparently does not occur during photolysis of azid-1 as the photoproduct has a mass consistent with the loss of $N_2$ and the reaction with a solvent water molecule. Perhaps cyclization does not occur because of the excessive ring strain generated from the fusion of three 5-membered heterocycles. Loss of $N_2$ and addition of solvent usually indicates ring expansion with phenyl azides, but this pathway is not consistent with the NMR of the product and its decreased affinity for $Ca^{2+}$. Ring expansion is well known to be hindered by ortho substituents as present in azid-1. Instead, rapid protonation by water of the strongly basic nitrene, **9** forms the nitrenium ion, **11** (Figure 4) within 1 ns as recently reported for aryl azides photolyzed in water [25]. Phenyl nitrenium ion reacts characteristically as the iminocyclohexadienyl cation producing 4-aminophenol in water by para attack of hydroxide or water followed by proton tautomerization [26]. A comparable resonance structure for the nitrenium ion formed from photolyzing azid-1 is **12**, in which the oxazole nitrogen bears the positive charge. Attack by hydroxide or water at the positive charge in either of these intermediates could occur resulting in either a vinylogous N-OH amidine (**14**) or a vinylogous N-H amidine (**16**) which would protonate (**2** and **18** respectively) at neutral pH with expected $pK_a$s > 9 [27]. As these products are isomers, they cannot be distinguished by mass. Determining the site of attachment of the N-OH group by $^1$H-NMR studies would be impossible in protic solvents as these protons rapidly exchange with the solvent. These two possible reaction pathways can be delineated by alkaline or mildly acidic hydrolysis of the imine bond in **14** or **16** to produce the two benzofuran-3-ones **20** or **22** respectively. Only the first route (i.e **14** to **20**) results in the change in mass of +1 found exclusively. Attack by solvent at the non-nitrene nitrogen is consistent with previous studies of phenyl azides [26] which photolyze solely to the analogous ring-substituted product (usually at the para position). With para-substituted phenyl azides, attack at this position leads to imine products which are susceptible to hydrolysis to substituted cyclohexadienones in a comparable manner to the photoproducts from azid-1. Further mass spectral results supporting this mechanism are peaks consistent with the addition of methanol when **1b** was photolyzed in aqueous methanol to form **15b** and subsequent hydrolysis to the corresponding N-methoxy benzofuran-3-one **21b**. These results do not rule out the possibility of subsequent rearrangement of **16** to **14** by hydroxyl migration between the imidine nitrogens although this appears unlikely as the methanol photoproduct would have to undergo intramolecular methoxy migration to produce exclusively **21b**. Similarly when azid-1 is photolyzed in methanol, the product binds $Ca^{2+}$ with a comparable affinity to **2a** as expected for the N-methoxy amidinium product **13a**. The rapid generation of **2**, complete within 2 ms, is not surprising considering the high reactivity of nitrenes and nitrenium ions with lifetimes in the nanosecond and microsecond range respectively [25]. Transient absorbance spectroscopy following laser flash photolysis could possibly detect these intermediates as well as the formation of the amidine and its protonation.

### Sensitivity to UV and two-photon photolysis

The high sensitivity of azid-1 to light is in agreement with numerous studies involving polycyclic aromatic azides which show quantum efficiencies approaching unity, particularly for the more extended ring structures [13]. In combination with the high extinction coefficients of the fura-2 stilbene-like chromophore, the light sensitivity (or the product of the extinction coefficient and the quantum yield at the wavelength of irradiation) of azid-1 greatly exceeds that of existing caged calciums by at least an order of magnitude (Table 1). When incorporated into Purkinje cells, azid-1 was able to mimic the action of nitr-7 in producing LTD but with up to tenfold briefer flashes of light. That yet briefer flashes were ineffectual and that more azid-1 was required (2 mM compared to 0.5 mM nitr-7) probably reflects the difference in chelator starting affinity.

Such enhanced photolability permits the use of less expensive flash lamps and lasers, allows more photorelease per flash, and reduces any deleterious effects of the UV light upon the biological sample. In addition, these more favorable optical properties of azid-1 greatly increase its ability to undergo two-photon photolysis compared to conventional nitrobenzyl based caged $Ca^{2+}$ (E.B. Brown, J.B. Shear, S.R.A., R.Y.T., W.W. Webb, unpublished observations). In this emerging and potentially powerful technique [10], two infra-red photons, if absorbed simultaneously, can elicit the same photoreaction as a single UV photon. The high photon density required for such a process confines two-photon photolysis to a volume of a few femtoliters in a tightly focused laser beam of femtosecond infra-red pulses, in comparison with conventional one-photon photolysis where photorelease occurs

throughout the beam. A high two-photon cross section is particularly important for a caged $Ca^{2+}$ as millimolar amounts may have to be photolyzed to overcome the intracellular $Ca^{2+}$ buffer compared to the micromolar or less amounts required for other caged compounds. The maximal two-photon cross section for azid-1 is ~1.4 GM (Göppert-Mayer; 1 GM = $10^{-50}$ $cm^4$·s/photon) at 700 nm, at least 100-fold greater than the value for DM–nitrophen (E.B. Brown, J.B. Shear, S.R.A., R.Y.T., W.W. Webb, unpublished observations). NP–EGTA has negligible cross section under these conditions. The high value for the cross section of azid-1 is not surprising considering the value of 12 GM for $Ca^{2+}$-bound fura-2 [28], which only differs by the absence of the azide group. The ability to restrict $Ca^{2+}$ elevations to precise subcellular locations will allow more accurate spatial probing of $Ca^{2+}$-dependent processes such as exocytosis and muscle contraction.

The high extinction coefficient of azid-1 could be a disadvantage in optically thick cells or tissue as inner-filtering could reduce the homogeneity of photorelease through the sample. The conventional caged $Ca^{2+}$ chelators suffer less from this particular problem particularly NP–EGTA which contains an unsubstituted nitrobenzyl group. However, photolyzing sufficient cage to generate the desired increase in $Ca^{2+}$ can then become difficult [29]. For two-photon photolysis, inner-filtering effects are negligible because all caged $Ca^{2+}$ have no absorbance in the infra red.

#### Comparison of azid-1 with other caged calciums

Azid-1 has several additional advantages over other caged $Ca^{2+}$ currently in use. The over 500-fold decrease in its $Ca^{2+}$ affinity from 0.23 μM to 120 μM upon photolysis should permit control of the many physiological events that are sensitive to changes in $[Ca^{2+}]_i$ in this range. In comparison, nitr-5 and nitr-7 permit only modest elevations in $Ca^{2+}$ of a few micromolar allowing only partial or no activation of some $Ca^{2+}$-sensitive processes, whereas DM–nitrophen and NP–EGTA can produce increases up to millimolar levels (Table 1). Azid-1 binds $Ca^{2+}$ more weakly before photolysis than the other caged $Ca^{2+}$s, however, so in cells with a typical resting $[Ca^{2+}]_i$ of 100 nM, less $Ca^{2+}$ will be bound and released upon irradiation. Furthermore, any unphotolyzed $Ca^{2+}$-free azid-1 will buffer the photoreleased ion (with the expected fast kinetics of BAPTA-based chelators of $> 10^8$ $M^{-1}$ $s^{-1}$) and limit the size of the $Ca^{2+}$ elevation. This problem is solved if the light flash is strong enough to photolyze both the $Ca^{2+}$-free as well as the $Ca^{2+}$-bound azid-1. Such complete photolysis is aided by the high quantum efficiency of unbound azid-1 and its absorbance at slightly longer wavelengths than the $Ca^{2+}$-complex. Another answer would be to increase the $Ca^{2+}$ affinity of azid-1 before photolysis by, for example, incorporation of a *cis*-cyclopentane ring into the ethane bridge between the two ether oxygens, as in nitr-7 [5]. This should strengthen the binding by a factor of 3–4 to a $K_d$ of 60–90 nM but would also presumably increase $Ca^{2+}$ binding of the photoproduct by a similar amount resulting in a lower final $[Ca^{2+}]$ after photolysis. Such modification (although requiring considerable organic synthesis) may be necessary for those applications in which free $[Ca^{2+}]$ must be kept particularly low before photolysis.

The proposed mechanism for azid-1 photolysis results in the uptake of one proton per $Ca^{2+}$ released. Increasing the pH in the cytoplasm of a cell is therefore a possible side-effect which should be controlled by the addition of pH buffer if the concentration of azid-1 is sufficiently high enough to overcome the strong intrinsic cytoplasmic $H^+$ buffer. A similar alkalinification is also shown by DM–nitrophen and NP–EGTA.

The presence of fluorescent impurities, such as 3-amino-fura-2, in preparations of azid-1 may complicate monitoring of photogenerated $Ca^{2+}$ increases inside cells using fluorescent $Ca^{2+}$ indicators. The impurity, being itself an emission-ratioable indicator like indo-1, could be used to follow $Ca^{2+}$ photorelease, except the high photosensitivity of azid-1 at the required excitation wavelength (about 350 nm) for 3-amino-fura-2 would cause slow release of $Ca^{2+}$ in the absence of a flash. Upon binding $Ca^{2+}$, 3-amino-fura-2 shifts emission from 490 to 420 nm so release of $Ca^{2+}$ by azid-1 results in fluorescent changes at these wavelengths that could interfere with signals from long wavelength fluorescent indicators such as fluo-3. Further purification of azid-1 following saponification may be necessary to prevent such cross talk.

The metal-binding site of azid-1 is based upon BAPTA or EGTA, (as is nitr-5, nitr-7 and NP–EGTA) and shows the greater than $10^4$ selectivity for $Ca^{2+}$ over $Mg^{2+}$ required for producing $Ca^{2+}$ increases without perturbing $Mg^{2+}$ levels under physiological conditions, unlike DM–nitrophen, which acts as a caged $Mg^{2+}$ and a caged $Ca^{2+}$. Like other BAPTA-based chelators, the $Ca^{2+}$ affinity of azid-1 shows little sensitivity to pH in the physiological range, and fast buffering kinetics (milliseconds), compared to caged $Ca^{2+}$ derived from EDTA (DM–nitrophen) and EGTA (NP–EGTA), which permit more efficient clamping of intracellular levels before and after photolysis. High on-rates for $Ca^{2+}$ binding are important to minimize the generation of transient spikes of high $[Ca^{2+}]$ lasting a few milliseconds following a flash that leaves sufficient $Ca^{2+}$-free chelator unphotolyzed to slowly re-bind part of the released $Ca^{2+}$. Transient $Ca^{2+}$ increases for DM–nitrophen and NP–EGTA have been measured directly using low-affinity fluorescent $Ca^{2+}$ indicators [30,31].

## Significance

**Rapid increases in levels of intracellular free calcium in the form of transients, oscillations and gradients have been described in many cells in response to a variety of**

stimuli. Fluorescent imaging of this ubiquitous second messenger has also revealed highly localized $Ca^{2+}$ elevations or local 'hot spots' within individual cells. Detailed mechanisms of the generation and control of $Ca^{2+}$ signals and their downstream biochemical effects are still poorly understood, however. One valuable technique used to probe and understand such pathways is the controlled spatial and temporal release of $Ca^{2+}$ by irradiation of photosensitive chelators or caged calciums. Here, we introduce such a photolabile chelator, azid-1, with new and useful properties, by a novel application of the photochemistry of azides to the design of photoreleasable or caged molecules. Azid-1 can selectively produce a photoinduced $Ca^{2+}$ increase to the 10–100 μM range from the typical cellular resting levels of 0.1–0.2 μM in the presence of, and without perturbing, physiological $Mg^{2+}$ concentrations. Such elevated intracellular free calcium is sufficient to activate most $Ca^{2+}$ triggered cellular processes, including muscle contraction and exocytosis of synaptic vesicles in neurons. Azid-1 is considerably more light sensitive than currently available caged calciums which should permit larger increases in $Ca^{2+}$ per flash, decrease any deleterious biological effects of UV irradiation, and allow photorelease of $Ca^{2+}$ by two-photon photolysis in volumes as small as a few femtoliters inside living cells. The technique of two-photon photolysis will enable direct probing of the role of $Ca^{2+}$ with unprecedented spatial resolution within individual cells.

## Materials and methods

### *Chemistry*

Chemicals (Aldrich; Milwaukee, WI, USA) and solvents (HPLC-grade, Fisher; Fair Lawn, NJ, USA) were used directly as received unless otherwise noted. Chloroform and dimethylformamide (DMF) were dried over 4 Å molecular sieve. Biochemicals were from Aldrich or Calbiochem (La Jolla, CA, USA).

Proton magnetic resonance spectra ($^1$H NMR) were recorded on a Gemini 200-MHZ spectrometer (Varian; Palo Alto, CA, USA) in $CDCl_3$ unless otherwise noted, and the chemical shifts are given in δ values relative to tetramethylsilane. Ultra-violet spectra were recorded on a Lambda Array 3840 spectrophotometer (Perkin-Elmer; Norwalk, CT, CA) or a Cary 3E UV-Visible spectrophotometer (Varian; Palo Alto, CA, USA) at 20°C. Electrospray mass spectrometry (5989B,Hewlett-Packard; Palo Alto, CA, USA) of **1b** and its photoproducts was performed by injecting ~1 mM solutions of the triethylammonium salt in $CH_3CN$-$H_2O$ and detecting negative ions.

TLC was carried out on precoated silica gel 60F-254 or reverse-phase RP-18, F-254 plates (E Merck, EM Separations; Gibbstown, NJ, USA). For column chromatography, silica gel 60 (230–400 mesh, E Merck) was used. All manipulations of compounds sensitive to near ultraviolet light were performed under an orange safety lamp.

### *Oxime* **4**

**3** [12] (1.0 g, 1.36 mmol) dissolved in dioxane (6 ml) and methanol (6 ml) was treated with a solution of hydroxylamine hydrochloride (278 mg, 4 mmol) and sodium acetate (230 mg, 2.8 mmol) dissolved in water (2.8 ml) at room temperature. After gentle warming to 60°C to dissolve any solids, the reaction mixture was kept overnight at room temperature. The product was precipitated by the addition of water (10 ml) and collected by filtration. Recrystallization from 95% ethanol yielded oxime **4** as white crystals, m.p. 108–110°C. Yield, 0.98 g (95%). $^1$NMR δ 1.16 (t, 12 H, $OCH_2CH_3$), 2.25 (s, 3H, $ArCH_3$), 4.05 (q, 4H, $OCH_2CH_3$), 4.07 (q, 4H, $OCH_2CH_3$), 4.12 (s, 2H, $NCH_2$), 4.14 (s, 2H, $NCH_2$), 4.24 (s, 4H, $OCH_2CH_2O$), 5.00 (s, 2H, benzyl $CH_2$), 6.39 (s, 1H, H-3), 6.7 (m, 3H, H-3′,4′,6′), 7.11 (s, 1H, oxime OH), 7.28 (s, 1H, H-6), 7.38 (m, 5H, benzene), 8.45 (s, 1H, CH=, syn). ES-MS (positive ion) [$CH_3CN$:$H_2O$; 95:5] 752.4 (M+1); calc'd M = 751.3.

### *Nitrile* **5**

A solution of **4** (0.98 g, 1.31 mmol) in chloroform (2 ml) was added in one portion to a suspension of phosgene iminium chloride (0.36 g, 2.2 mmol) in chloroform (5 ml). After 10 min reflux, during which HCl fumes were evolved, the resulting solution was evaporated to dryness, and the residue boiled with methanol (50 ml). After cooling in ice, **5** was collected by filtration and washed with several portions of cold methanol. Yield 0.83 g (87%). M.p. 145–146°C. $^1$NMR δ 1.16 (t, 6H, $OCH_2CH_3$), 1.17 (t, 6H, $OCH_2CH_3$), 2.26 (s, 3H, $ArCH_3$), 4.06 (q, 4H, $OCH_2CH_3$), 4.07 (q, 4H, $OCH_2CH_3$), 4.11 (s, 8H, $NCH_2$), 4.20 (s, 4H, $OCH_2CH_2O$), 5.12 (s, 2H, benzyl $CH_2$) 6.31 (s, 1H, H-3), 6.6-6.8 (m, 3H, H-3',4',6'), 7.00 (s, 1H, H-6), 7.39 (m, 5H, benzene). ES-MS (positive ion) [$CH_3CN$:$H_2O$; 95:5] 734.4 (M+1); calc'd M = 733.3.

### *Salicylnitrile* **6**

**5** (300 mg, 0.41 mmol) was catalytically hydrogenated at room temperature and pressure with 300 mg of 5% Pd/C in ethyl acetate:acetic acid (25 ml, 1:2 v/v). Uptake was complete in 30 min: the reaction mixture was filtered and evaporated to dryness to yield the product, **6**. Recrystallization from ethanol gave a pale yellow solid, m.p. 139–141°C. Yield 226 mg (86%). $^1$NMR δ 1.17 (t, 6H, $OCH_2CH_3$), 1.19 (t, 6H, $OCH_2CH_3$), 1.55 (br s,~2H, OH and DOH), 2.26 (s, 3H, $ArCH_3$), 4.08 (q, 4H, $OCH_2CH_3$), 4.09 (q, 4H, $OCH_2CH_3$), 4.12 (s, 4H, $NCH_2$), 4.18 (s, 4H, $NCH_2$), 4.21 (s, 4H, $OCH_2CH_2O$), 6.27 (s, 1H, H-3), 6.6–6.8 (m, 3H, H-3′,4′,6′), 6.90 (s, 1H, H-6). ES-MS (positive ion) [$CH_3CN$:$H_2O$; 95:5] 644.3 (M+1); calc'd M = 643.3.

### *3-Amino-2-oxazolylbenzofuran* **7**

**6** (100 mg, 0.155 mmol), ethyl 2-(chloromethyl)oxazole-5-carboxylate (30 mg, 0.16 mmol; prepared as described [12]) and anhydrous potassium carbonate (30 mg, 0.22 mmol) were heated in dry DMF (0.25 ml) at 130°C for 1 h under an argon atmosphere. The cooled reaction mixture was diluted with water (5 ml), acidified with acetic acid and extracted (3 x 5 ml) with ethyl acetate. After drying over sodium sulfate, the extract was evaporated to dryness to yield crude **7**, that was further purified by silica gel chromatography eluting with ethyl acetate/hexane. The resulting yellow solid was triturated with isopropyl ether and filtered. Yield 71 mg (61%). M.p. 83–85°C. $^1$NMR δ 1.16 (t, 6H, $OCH_2CH_3$), 1.21 (t, 6H, $OCH_2CH_3$), 1.40 (t, 3H, oxazole $OCH_2CH_3$), 2.26 (s, 3H, $ArCH_3$), 4.06 (q, 4H, $OCH_2CH_3$), 4.12 (q, 4H, $OCH_2CH_3$), 4.15 (s, 4H, $NCH_2$), 4.20 (s, 4H, $NCH_2$), 4.3 (dt, 4H, $OCH_2CH_2O$), 4.41 (q, 2H, oxazole $OCH_2CH_3$), 5.09 (s, 2H, $NH_2$), 6.67–6.81(m, 3H, H-3′,4′,6′), 6.88 (s, 1H, H-7), 7.14 (s, 1H, H-4), 7.85 (s, 1H, oxazole). ES-MS (positive ion) [$CH_3CN$:$H_2O$; 95:5] 797.3 (M+1); calc'd M = 796.3.

### *Azid-1 pentaethyl ester* **8**

**7** (20 mg, 26.4 μmol) was dissolved in cold glacial acetic acid (300 μl) and added dropwise with stirring to a solution of nitrosyl hydrogensulfate (20 mg, 157 μmol, Lancaster Synthesis; Windham, NH, USA) in concentrated sulfuric acid (200 μl) at 0°C. After 20 min, the reaction mixture was added dropwise to a ice-cold saturated aqueous solution of sodium azide (20 ml) with vigorous stirring (CARE; hydrazoic acid generated; carry out in well-ventilated fumehood). After neutralization with solid sodium bicarbonate, the mixture was diluted with water and extracted (3 x 20 ml) with ethyl acetate. Drying over sodium sulfate and evaporation to dryness yielded crude **8** which was further purified by silica gel column chromatography eluting with ethyl acetate/hexane followed by trituration with ethanol. Yield of pale yellow solid, 13.5 mg (66 %). M.p. 114–116°C. $^1$NMR δ 1.16 (t, 6H, $OCH_2CH_3$), 1.18 (t, 6H, $OCH_2CH_3$), 1.42 (t, 3H, oxazole $OCH_2CH_3$), 2.27 (s, 3H, $ArCH_3$),

4.05 (q, 8H, $OCH_2CH_3$), 4.12 (s, 4H, $NCH_2$), 4.22 (s, 4H, $NCH_2$), 4.32 (s, 4H, $OCH_2CH_2O$), 4.43 (q, 2H, oxazole $OCH_2CH_3$), 6.70-6.80 (m, 3H, H–3′,4′,6′), 6.95 (s, 1H, H–7), 7.13 (s, 1H, H-4), 7.91 (s, 1H, oxazole). ES-MS (positive ion) [$CH_3CN$:$H_2O$; 95:5] 823.2 (M+1); calc'd M = 822.3.

### *Azid-1 pentapotassium salt* ***1b***

Azid-1 pentaethyl ester **8** (6.71 mg, 8.15 μmol) was saponified to the penta-anion by dissolution in dioxane (0.2 ml) and methanol (0.2 ml), followed by addition of aqueous 1M potassium hydroxide (79 μl, 79 μmol) and keeping at room temperature overnight. The organic solvents were evaporated under a stream of $N_2$ at room temperature and the resulting solution neutralized to pH~7 with a solution of an appropriate acid such as MOPS or HCl. Alternatively the free acid can be precipitated by the addition of dilute hydrochloric acid to pH 2, cooling on ice and collecting the resulting pale yellow precipitate by centrifugation. Addition of the calculated amount (i.e. 5 equivalents) of aqueous KOH generates the pentapotassium salt. Solutions were kept frozen between use and only handled under orange safety light or subdued lighting. $^1$NMR $D_2O$ δ 2.25 (s, 3H, $ArCH_3$), 3.72 (s, 4H, 2′-$NCH_2$), 3.85 (s, 4H, 6-$NCH_2$) 4.40 (s br, 4H, $OCH_2CH_2O$), 6.77 (s, 2H, H–3′,4′), 6.95, (s, 1H, H–6′), 6.99 (s, 1H, H–7), 7.32 (s, 1H, H–4), 7.64 (s, 1H, oxazole).

### *$^1$NMR of photolysis product*

Azid-1 pentaethyl ester (5 mg, 6 μmol) was saponified as described above and adjusted to pH 7 with dilute hydrochloric acid. The solution was evaporated to dryness and then repeatedly (two to three times) redissolved in $D_2O$ (0.5 ml) and re-evaporated. Photolysis was accomplished by irradiation for 5 min with a Spectroline TC-365A UV transilluminator (Spectronics Corp; Westbury, NY, CA). $^1$NMR $D_2O$ δ 2.21 (s, 3H, $ArCH_3$), 3.77 (s, 4H, 2′-$NCH_2$), 4.08 (s br, 4H, $OCH_2CH_2O$),4.27 (s, 4H, 6-$NCH_2$), 5.91 (s, 1H, H-7), 6.65 (dd, 2H, H–3′,4′), 6.91 (s, 1H, H–6′), 7.25 (s, 1H, H–4), 7.45 (s, 1H, oxazole).

### *Calcium and magnesium affinities*

$Ca^{2+}$-binding constants for azid-1 before photolysis were determined by monitoring UV-visible spectra during titration of EGTA buffers to varying free $Ca^{2+}$ levels by the reciprocal dilution method [5]. The dissociation constants of Ca·EGTA were calculated as previously described [32]. Photolyzed azid-1 was titrated by adding aliquots of standard solutions of $CaCl_2$ to a nominally $Ca^{2+}$-free solution in which the $Ca^{2+}$ contamination present initially in the solution before titration was negligible (less than a few micromolar). Hill plots of the resulting spectral changes against -log[$Ca^{2+}$] gave the dissociation constants as x intercepts with gradients of 1.01 ± 0.01 and 0.96 ± 0.01 for azid-1 and the photoproduct respectively, indicating a 1:1 complex of the chelator and $Ca^{2+}$ is formed.

Free [$Mg^{2+}$] was likewise controlled by Mg/EGTA buffers, assuming an apparent dissociation constant for Mg·EGTA complex (including its monoprotonated form) of 6 mM at pH 7.60 in 0.1 M ionic strength [32].

### *Quantum efficiency of photolysis*

The photolysis quantum efficiencies of azid-1 was determined by alternately irradiating a buffered solution of the substrate containing zero (1 mM EDTA) or saturating $Ca^{2+}$ with a known intensity of near-UV light and recording the resulting absorbance spectrum in a spectrophotometer as described previously [5]. A B-100 Mercury lamp (Spectronics Corp; Westbury, NY, CA) was used as a source of 365 nm light and its intensity (~$1–2 \times 10^{-8}$ einsteins $cm^{-2}$ $s^{-1}$) measured each experimental day by actinometry using 6 mM potassium ferrioxalate [33].

### *Flash photolysis*

Flash photolysis of azid-1 and the concomitant monitoring of free $Ca^{2+}$ concentration with fluo-3, a fluorescent $Ca^{2+}$-indicator, were performed using methodology and instrumentation described previously [34] except a flash-lamp was used for photorelease. Briefly, output from a 150 W Xe arc lamp was passed through a grating monochromator to yield the 490 nm light used to probe the fluo-3 indicator. The fluo-3 intensity from droplets (~50–100 μm diameter) of buffered aqueous solutions of part $Ca^{2+}$-loaded azid-1 and fluo-3 (0.65 mM azid-1, 0.5 mM $CaCl_2$, 0.1 mM fluo-3, 25 mM $KPO_4$ pH 7.2) prepared using a glass microinjection pipet, under mineral oil on a IM-35 inverted fluorescence microscope stage (Zeiss; Thornwood, NY, USA) was recorded by a photomultiplier and processed by a DM3100 fluorimeter (Spex; Edison, NJ, USA). Photolyses were performed by triggering a Strobex 238 xenon flash lamp (Chadwick Helmuth; El Monte, CA, USA) through a UV UG-1 bandpass filter (Rolyn Optics; Covina, CA, USA) placed in the excitation path of the Zeiss fluorescence microscope. A custom dichroic mirror (DR 505LP UV-enhanced, Omega; Battleboro, VT, USA) was placed in the microscope epifluorescence filter cube to reflect both UV and 490 nm light while retaining transmission at wavelengths > 510 nm, where fluo-3 emits strongly. The time resolution of this apparatus was limited by the 2 ms acquisition time of the fluorimeter.

### *Biological tests*

Electrophysiological recordings from Purkinje cells in cerebellar brain slices freshly prepared from young adult rats were performed as described previously [16]. Photolytic illumination was provided by a 200 W DC mercury arc lamp with an electromechanical shutter, focused through the epi-illumination pathway of an Axioplan microscope (Zeiss; Thornwood, NY, USA) with a 10 × water-immersion objective. Photolytic flashes were 100 ms at 1 Hz for 30 s. Inner-filtering (from azid-1 and some tissue opacity to UV) is unlikely to occur at the site of LTD induction in the dendrites with a total thickness of a few μm in these sagittal slices. It is possible this may slightly limit the extent of photolysis in the cell body with a diameter of 20–40 μm . The intracellular pipette solution contained: 130 mM $K^+CH_3SO_3^-$, 10 mM KCl, 10 mM K HEPES, 4.6 mM $MgCl_2$, 4 mM Na ATP, 1 mM Na GTP, 1 mM EGTA, 16 mM sucrose, and 2 mM azid-1 at pH 7.35 and 295 mOsmol.

## Acknowledgements

We are grateful to Alec Harootunian for his help with the flash photolysis experiments and Larry Gross for mass spectroscopy. This work was supported by NIH grant NS27177 and the Howard Hughes Medical Institute.

## References

1. Adams, S.R. & Tsien, R.Y. (1993). Controlling cell chemistry with caged compounds. *Annu. Rev. Physiol.* **55**, 755-784.
2. Kao, J.P.Y. & Adams, S.R. (1993). Photosensitive caged compounds: design, properties, and biological applications. In *Optical Microscopy: Emerging Methods and Applications.* (Herman, B. and Lemasters, J.L. eds), pp. 27-85, Academic Press, New York.
3. Zucker, R.S. (1994). Photorelease techniques for raising or lowering intracellular $Ca^{2+}$. *Methods Cell Biol.* **40**, 31-63.
4. Kaplan, J.H. (1990). Photochemical manipulation of divalent cation levels. *Annu. Rev. Physiol.* **52**, 897-914.
5. Adams, S.R., Kao, J.P.Y., Grynkiewicz, G., Minta, A. & Tsien, R.Y. (1988). Biologically useful chelators that release $Ca^{2+}$ upon illumination. *J. Am. Chem. Soc.* **110**, 3212-3220.
6. Ellis-Davies, G.C.R. & Kaplan, J.H. (1988). A new class of photolabile chelators for the rapid release of divalent cations: generation of caged Ca and caged Mg. *J. Org. Chem.* **53**, 1966-1969.
7. Ellis-Davies, G.C.R. & Kaplan, J.H. (1994). Nitrophenyl-EGTA, a photolabile chelator that selectively binds $Ca^{2+}$ with high affinity and releases it rapidly upon photolysis. *Proc. Natl Acad. Sci. USA* **91**, 187-191.
8. Wootton, J.F. & Trentham, D.R. (1989). 'Caged' compounds to probe the dynamics of cellular processes: synthesis and properties of some novel photosensitive P-2-nitrobenzyl esters of nucleotides. In *NATO Advanced Research Workshop on Photochemical Probes in Biochemistry.* (Nielsen, P.E. ed.), pp. 277-296, Kluwer Academic Publishers, Boston.
9. McCray, J.A. & Trentham, D.R. (1989). Properties and uses of photoreactive caged compounds. *Annu. Rev. Biophys. Biophys. Chem.* **18**, 239-270.
10. Denk, W., Strickler, J.H. & Webb, W.W. (1990). Two-photon laser scanning fluorescence microscopy. *Science* **248**, 73-76.

11. Zucker, R.S. (1996). Exocytosis: a molecular and physiological perspective. *Neuron* **17**, 1049-1055.
12. Grynkiewicz, G., Poenie, M. & Tsien, R.Y. (1985). A new generation of $Ca^{2+}$ indicators with greatly improved fluorescence properties. *J. Biol. Chem.* **260**, 3440-3450.
13. Reiser, A. & Wagner, H.M. (1971). Photochemistry of the azido group. In *The Chemistry of the Azido Group.* (Patai, S. ed.), pp. 441-501, Wiley, New York.
14. Staros, J.V., Bayley, H., Standring, D.N. & Knowles, J.R. (1978). Reduction of aryl azides by thiols: implications for the use of photoaffinity reagents. *Biochem. Biophys. Res. Comm.* **80**, 568-572.
15. Eberhard, M. & Erne, P. (1989). Kinetics of calcium binding to fluo-3 determined by stopped-flow fluorescence. *Biochem. Biophys. Res. Comm.* **163**, 309-314.
16. Lev-Ram, V., Makings, L.R., Keitz, P.F., Kao, J.P.Y. & Tsien, R.Y. (1995). Long-term depression in cerebellar Purkinje neurons results from coincidence of nitric oxide and depolarization-induced $Ca^{2+}$ transients. *Neuron* **15**, 407-415.
17. Lev-Ram, V., Jiang, T., Wood, J., Lawrence, D.S. & Tsien, R.Y. (1997). Synergies and coincidence requirements between NO, cGMP, and $Ca^{2+}$ in the induction of cerebellar long-term depression. *Neuron* **18**, 1025-1038.
18. Adams, S.R., Kao, J.P.Y. & Tsien, R.Y. (1989). Biologically useful chelators that take up $Ca^{2+}$ upon illumination. *J. Am. Chem. Soc.* **111**, 7957-7968.
19. Thirlwell, H., Corrie, J.E.T., Reid, G.P., Trentham, D.R. & Ferenczi, M.A. (1994). Kinetics of relaxation from rigor of permeabilized fast-twitch skeletal fibers from the rabbit using a novel caged ATP and apyrase. *Biophys. J.* **67**, 2436-2447.
20. Bayley, H. & Knowles, J.R. (1977). Photoaffinity labeling. *Methods Enzymol.* **46**, 69-114.
21. Schuster, G.B. & Platz, M.S. (1992). Photochemistry of phenyl azide. *Adv. Photochem.* **17**, 69-143.
22. Barton, D.H.R., Sammes, P.G. & Weingarten, G.G. (1971). Photochemical transformations. Part XXVIII. Aryl azides as potential photosensitive protecting groups. *J. Chem. Soc. (C)* 721-728.
23. Dyall, L.K. (1983). Pyrolysis of aryl azides. In *The Chemistry of Halides, Pseudo-halides and Azides, part 1.* (Patai, S. and Rappoport, Z. eds), pp. 287-320, Wiley, New York.
24. Smith, P.A.S., Budde, G.F. & Chou, S.S.P. (1985). Comparison of the ease of thermolysis of ortho-substituted phenyl azides having $\alpha$, $\beta$ or $\beta$, $\gamma$ imine function. *J. Org. Chem.* **50**, 2062-2066.
25. McClelland, R.A. (1996). Flash photolysis generation and reactivities of carbenium ions and nitrenium ions. *Tetrahedron* **52**, 6823-6858.
26. McClelland, R.A., Kahley, M.J., Davidse, P.A. & Hadzialic, G. (1996). Acid-base properties of arylnitrenium ions. *J. Am. Chem. Soc.* **118**, 4794-4803.
27. Oszczapowicz, J. (1991). Basicity, H-bonding, tautomerism and complex formation of imidic acid derivatives. In *The Chemistry of Amidines and Imidates, Volume 2.* (Patai, S. and Rappoport, Z. eds), pp. 625-688, Wiley & Sons, New York.
28. Xu, C., Zipfel, W., Shear, J.B., Williams, R.M. & Webb, W.W. (1996). Multiphoton fluorescence excitation: new spectral windows for biological nonlinear microscopy. *Proc. Natl Acad. Sci. USA* **93**, 10763-10768.
29. Parsons, T.D., Ellis-Davies, G.C.R. & Almers, W. (1996). Millisecond studies of calcium-dependent exocytosis in pituitary melanotrophs: comparison of the photolabile calcium chelators nitrophenyl-EGTA and DM-nitrophen. *Cell Calcium* **19**, 185-192.
30. Escobar, A.L., Cifuentes, F. & Vergara, J.L. (1995). Detection of $Ca^{2+}$-transients elicited by flash photolysis of DM-nitrophen with a fast calcium indicator. *FEBS Lett.* **364**, 335-338.
31. Ellis-Davies, G.C.R., Kaplan, J.H. & Barsotti, R.J. (1996). Laser photolysis of caged calcium: rates of calcium release by nitrophenyl-EGTA and DM-nitrophen. *Biophys. J.* **70**, 1006-1016.
32. Tsien, R.Y. & Zucker, R.S. (1986). Control of cytoplasmic calcium with photolabile tetracarboxylate 2-nitrobenzhydrol chelators. *Biophys. J.* **50**, 843-853.
33. Hatchard, C.G. & Parker, C.A. (1956). A new sensitive chemical actinometer. II. Potassium ferrioxalate as a standard chemical actinometer. *Proc. R. Soc. Lond. A* **235**, 518-536.
34. Kao, J.P.Y., Harootunian, A.T. & Tsien, R.Y. (1989). Photochemically generated cytosolic calcium pulses and their detection by fluo-3. *J. Biol. Chem.* **264**, 8179-8184.
35. Martell, A.E. & Smith, R.M. (1974). *Critical Stability Constants, volume 1.* Plenum, New York.